THE COMPUTATION OF FLOW AND HEAT TRANSFER THROUGH SQUARE-ENDED U-BENDS, USING LOW-REYNOLDS-NUMBER MODELS

Konstantinos-Stephen P. Nikas
Department of Mechanical Engineering
UMIST, Manchester, UK
mcjtpn4@fluid.mech.ntua.gr

Hector Iacovides
Department of Mechanical Engineering
UMIST, Manchester, UK
h.iacovides@umist.ac.uk

ABSTRACT

This study considers the computation of turbulent flow and heat transfer in square-ended U-bends of strong curvature. Flows at two Reynolds numbers have been computed, one at 100,000 and one at 36,000 and in the thermal analysis the Prandtl number was either 5.9 (water) or 0.72 (air). The turbulence modelling approaches examined include a zonal and a low-Re k-ε model, a zonal and a low-Re basic DSM model and a realisable, wall-parameter-free second-moment closure. For the low-Re EVM and DSM models, an alternative length-scale correction term, independent of wall distance, has also been tested. All models produce similar flow predictions, suggesting that the flow development is mainly influenced by mean flow parameters rather than the turbulence field. The main flow features are reproduced, but predictive deficiencies after the 90° location have also been identified. The heat transfer comparisons, on the other hand, show that the low-Re DSM model with the alternative length scale correction produces the most reliable Nusselt number predictions for the Prandtl numbers examined.

INTRODUCTION

Flow and heat transfer through tight square-ended U-bends, shown in Figure 1, provide an idealised representation of the flow and thermal processes present in internal cooling passages of gas-turbine blades.. The flow development and the heat transfer characteristics inside these cooling passages are complex and highly three-dimensional, influenced by the presence of sharp U-bends, artificial rib-roughness and the rotation of the blades. For these reasons, flow and thermal development through blade cooling passages have been the subject of a number of investigations such as those of Metzger and Sahm (1986), Ekkad and Han (1995) and Rigby et al (1996)

In three-dimensional flows through curved ducts of moderate curvature, the primary influence on the flow development is the secondary motion. This is a mean flow phenomenon and can thus be reproduced by effective-viscosity models. Because, however, the secondary motion is generated within the boundary layers, one would expect that only turbulence models that resolve the near-wall motion would be able to reproduce the correct flow and thermal development. This has been shown to be the case by the work of Choi et al (1989) who instead of using the high-Re turbulence models with the wall-function approximation, adopted a zonal approach which allows the mean flow equations to be integrated up to the wall, using simple models of near-wall turbulence. Choi et al also showed that replacement of the high-Re k-ε in the duct core with an algebraic second-moment closure resulted in further improvements in the predicted flow field. Iacovides et al (1996a) subsequently showed that the introduction of a realisable, wall-parameter-free second-moment closure produced marked improvements in the predicted thermal development.

For U-ducts of curvature strong enough to cause flow separation, strong pressure gradients present at the bend entry and exit also exercise a strong influence. Bo et al. (1995) and Iacovides et al. (1996b) computed flow and heat transfer through a rounded-ended U-bend of a strong curvature ($R_c/D=0.65$), shown in Figure 1. The former study demonstrated that to obtain numerically accurate solutions, bounded high-order discretisation schemes had to be employed for convection of the turbulent variables (k and ε) as well as the mean flow variables, while the latter study suggested that, over the inner

wall, the modelling of turbulence anisotropy in the near-wall sub-layers, is of great importance in the prediction of the mean flow development. Both those investigations predicted that separation along the inner wall of the bend occurs later than what is indicated by the experimental data, though use of second-moment closures led to considerable improvements.

The question therefore arises as to whether the conclusions reached from the above numerical studies of curved U-bends are also applicable to square-ended U-bends. The recent emergence of local flow and thermal data for square-ended U-bends from our and also other groups, Iacovides et al. (1999), Ekkad & Han (1994), provided the validation data necessary to answer this question and led to the present study. The primary objective here is to assess the effectiveness of low-Re models similar to those we previously applied to flow computations through round-ended U-bends, while a further objective has been to introduce and assess the effectiveness of a recently developed realisable second-moment closure, Craft (1998).

THEORETICAL MODEL

The Reynolds-averaged flow equations are presented here in Cartesian tensor notation.

Continuity:
$$\frac{\partial}{\partial x_i}\left(\rho U_i\right) = 0 \qquad (1)$$

Momentum
$$\frac{\partial}{\partial x_j}\left(\rho U_j U_i\right) = -\frac{\partial P}{\partial x_i} + \frac{\partial}{\partial x_j}\left[\mu\left(\frac{\partial U_i}{\partial x_j} + \frac{\partial U_j}{\partial x_i}\right) - \rho\overline{u_i u_j}\right] \qquad (2)$$

Energy
$$\frac{\partial}{\partial x_j}\left(\rho\Theta\right) = \frac{\partial}{\partial x_j}\left(\frac{\mu}{Pr}\frac{\partial\Theta}{\partial x_j} - \rho\overline{u_j\theta}\right) \qquad (3)$$

Turbulence Modeling

Due to space limitations, the full set of the equations involved in the models used to obtain the Reynolds stresses and turbulent heat fluxes that appear in equations (2) and (3) respectively, cannot be included.

The turbulence models tested are the following:

1. A zonal effective-viscosity model (EVM)
2. The Launder-Sharma low-Re EVM.
3. A zonal basic differential stress model (DSM)
4. A basic low-Re DSM
5. The Craft realisable low-Re DSM

The zonal EVM consists of the standard high-Re k-ε in the duct core, matched to Wolfshteins's (1969) one-equation model in the near-wall regions. In the two basic DSM closures, the original equations of stress transport that include the linear pressure strain term, isotropic dissipation and wall-reflection terms have been further extended so that they can be used across the wall sub-layer. In the zonal DSM the near-wall dissipation rate is obtained from a prescribed length scale, while in the low-Re basic DSM the Launder-Sharma form of the dissipation rate equation is employed. A full set of the equations involved in the two EVM and the basic DSM models can be found in Iacovides and Raisee (1999).

In the computation of recirculating flows, the Launder-Sharma form of the dissipation rate equation requires the use of a length-scale correction term. Here, in addition to the term proposed by Yap (1987), which includes the wall distance, a recent version proposed by Iacovides and Raisee (1999), in which the resultant gradient of the turbulent length scale replaces the wall distance, has also been tested.

The Craft low-Re DSM model is a recent closure that includes a cubic form of the pressure strain term, does not rely on wall reflection terms and at the wall satisfies the two-component limit of turbulence.

In the EVM models the turbulent heat fluxes are modeled through the effective diffusivity approximation, while in all DSM models the generalised gradient diffusion hypothesis was used.

Numerical Aspects.

A three-dimensional non-orthogonal finite volume solver, STREAM, has been employed, developed at UMIST, which employs the Cartesian velocity decomposition. A collocated grid is used. The SIMPLE algorithm is employed for the calculation of the pressure field, with the Rhie and Chow flux modification. In the case of the DSM models the apparent viscosity concept is used to prevent numerical oscillations that arise from the explicit presence of the Reynolds stress gradients in the momentum equations. For the convective discretisation of all transport equations a bounded form of the quadratic upstream interpolation scheme (QUICK), was used, proposed by Iacovides (1999).

PRESENTATION AND DISCUSSION OF RESULTS.

As shown in Figure 1, the flow geometry is that of a square-ended U-bend of square cross-section in the straight tangents, with a ratio of 0.15 between the radius of the inner wall and the duct diameter. The flow domain started three duct diameters before the bend entry and extended to nine diameters afer its exit Two grids have been employed, the first consisting of 31x58 grid nodes over the half cross-section and 104

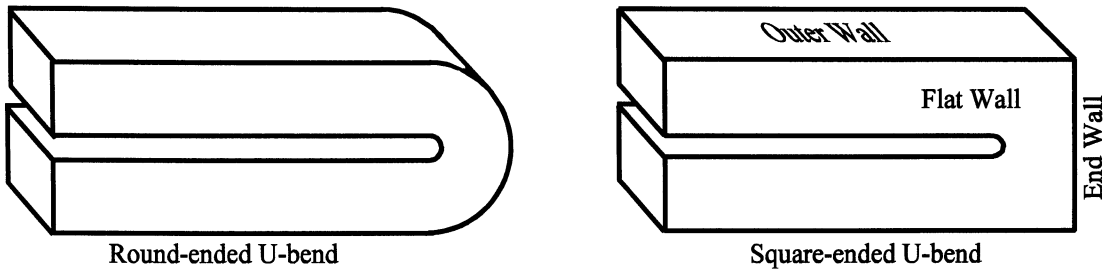

Figure 1. Flow Geometry

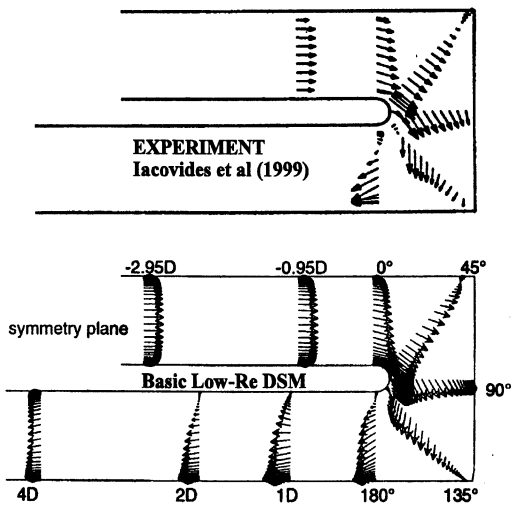

Figure 2. Comparison between computed and measured mean flow fields along the duct symmetry plane.

planes in the streamwise direction and the second consisting of 45x86x104 grid nodes. Computations have been carried out at two flow Reynolds numbers, 36,000 and 100,000. Heat transfer computations have been obtained with constant wall heat flux boundary conditions, at Prandtl number values of 0.72 and 5.9. At Pr=0.72 all duct walls were heated, while at Pr=5.9 only the two flat walls were heated, in order to be consistent with the experimental conditions. Fully developed duct flow hydrodynamic and thermal entry conditions have been prescribed, generated through preliminary computations.

Comparisons of the mean velocity field along the duct symmetry plane, shown in Figure 2, indicate that the main flow features present in the measurements are reproduced by the low-Re DSM, but with a narrower than measured separation bubble along the inner wall. The other models, not shown here, return a mean flow field similar to that of the low-Re DSM, apart from the realisable DSM that produces a slower recovery after the bend exit. Detailed mean flow comparisons are provided by the profiles of the streamwise velocity in Figure 3. The differences between the k-ε and DSM predictions are smaller than those identified in our studies of round-ended U-bends, Iacovides et al (1996b). This suggests that mean flow effects, such as the strong streamwise pressure gradients caused by the change in cross-sectional area around the bend, are more influential in square-ended U-bends. The failure of all models to predict the correct size of the separation bubble at the bend exit is evident, while the differences between the predictions of the realisable DSM and those of the other models in the first two downstream diameters, are also noticeable. Comparisons further downstream, not shown here, suggest that the slower downstream recovery produced by the realisable DSM is in contrast to the measured behaviour.

Figure 4 compares the computed development of the secondary motion within the bend with that inferred from the available measurements. The data show that the classical two-vortex structure prevails throughout the turn, with the vortices becoming more intense at the 90° plane, where the cross-sectional area is narrowest. The measurements also show that the flow within the bend is significantly non-symmetric. Flow visualisation tests, Iacovides et al (1999), showed that

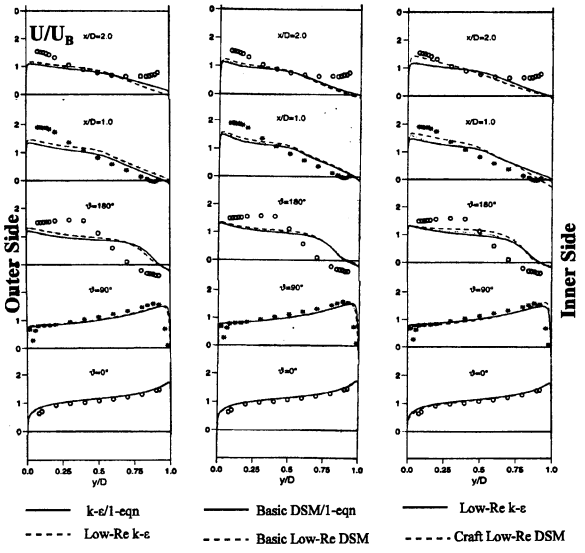

Figure 3. Comparison between computed and measured profiles of the axial velocity along duct symmetry plane.

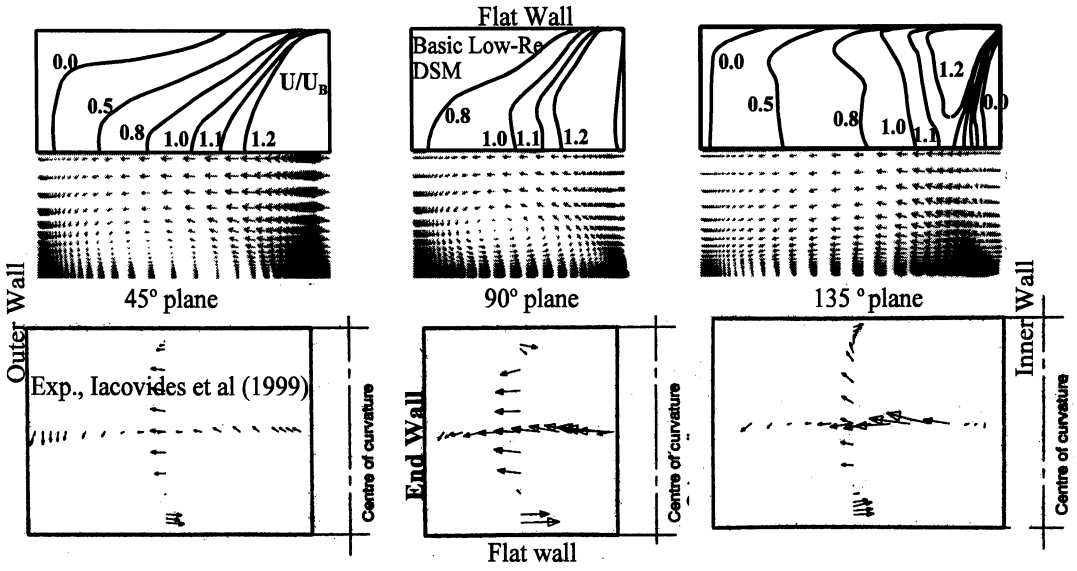

Figure 4. Comparison between predicted and measured cross-duct flow fields within the turn.

non-symmetry is caused by flow instabilities within the bend, which die down after the bend exit. The present computations assume both symmetry and steady conditions and consequently cannot reproduce this phenomenon. At the 45° and 90° planes the DSM computations reproduce the two-vortex structure. At the 135° plane, in contrast to the measurements, the computations show that almost over the entire cross-section the cross-duct motion is predominantly in the outward direction. This disappearance, from the predictions, of the two-vortex structure, appears to be caused by the fact that the boundary layer along the flat walls is suppressed, resulting in an almost two-dimensional variation of axial velocity from the inner to the outer wall. The Craft DSM closure, not included here, returns a weaker secondary motion, which is consistent with the generally slower flow development returned by this model. The other models, also not shown here, produce mean flow predictions similar to those of the basic low-Re DSM.

The profiles of the streamwise turbulence intensity, shown in Figure 5, reveal that all models severely under-predict intensity levels at and immediately after the bend exit. One possible explanation may be that the measured intensities also include the effects of the large-scale instabilities observed within the turn. Within the turn, the EVM models return higher intensities than the basic DSM closures, while after the turn the situation is reversed. The realisable Craft model, produces intensity distributions similar to those of the basic DSM, but somewhat lower levels.

Heat transfer computations on the other hand, such as the ones presented in Figure 6, for a Prandtl number of 0.72, show greater sensitivity to the turbulence models employed. The side-averaged Nusselt number measurements in Figure 6 were obtained at a Reynolds number of 60,000, while the predicted values were for an Re value of 100,000 and were then scaled for a value of 60,000 through the Dittus Boelter formula. All the models under-predict Nu levels within and after the bend. Not surprisingly the zonal models, especially the zonal k-ε, return the lowest Nu levels. There is relatively little difference between the low-Re predictions produced by the two alternative versions of the Yap term, especially for the basic DSM, with the predictions of the basic DSM marginally closer to the data than those of the low-Re k-ε. The realisable (Craft) DSM, while predicting reasonable Nu levels after the bend, within the bend

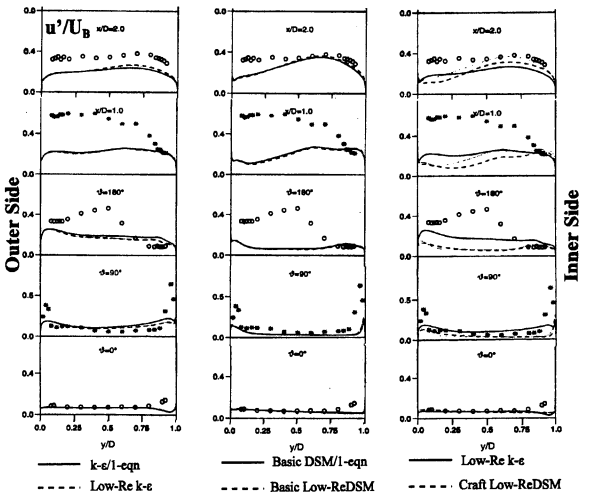

Figure 5. Comparison between computed and measured profiles of the axial component of turbulence intensity along symmetry plane

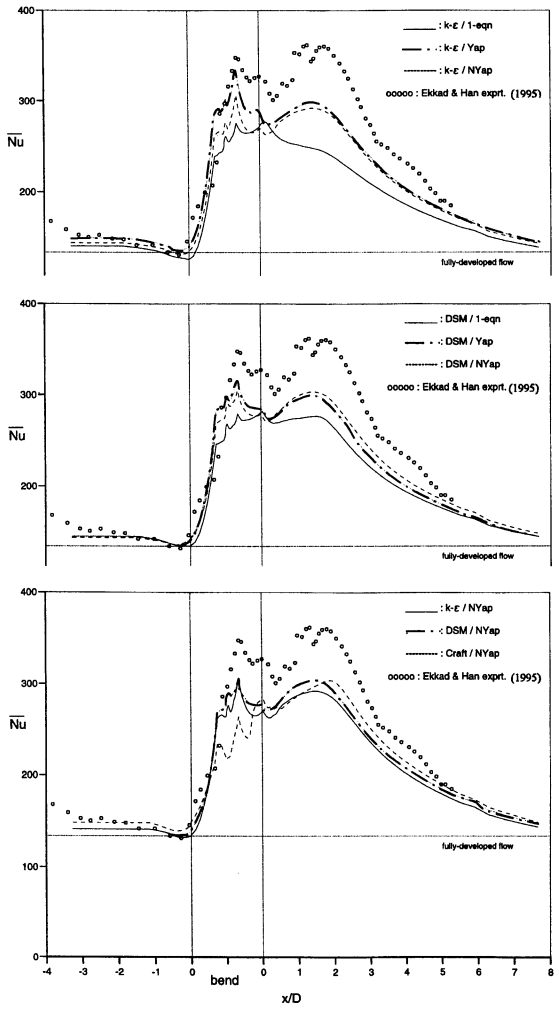

Figure 6. Comparisons of the axial variation of the side-averaged Nusselt number along the flat wall. Re=60,000 and Pr=0.72

severely under-predicts the Nusselt number.

Comparisons between the measured contours of the local Nusselt number and those predicted by the basic DSM with the differential version of the Yap term are shown in Figure 7. The measurements show that the Nusselt number starts to increase as the fluid enters the turn and that a local peak is reached over the first half of the turn, near the end wall. This Nu peak must be caused by impingement on the end wall. Over the second half of the turn, there is local minimum at the corner between the end and the outer walls. At the bend exit, the measured Nusselt number is high along the outer side, where the flow accelerates, and low along the inner side where there is a separation bubble. Further downstream, the high Nusselt number levels along the outer side spread over the entire flat wall, while after the first three downstream diameters, the measured Nusselt number starts to fall. Most of these features are returned by this model and overall Nusselt number levels are well predicted. The model fails to return the low Nu levels at the downstream corner of the bend, a feature consistent with the erroneous prediction of the outward motion at the 135° plane, identified in Figure 4. Moreover, the predictions show a slower rise in Nusselt number at the bend entry, larger regions of high Nu levels in the bend and downstream and also a larger region of low Nu levels along the inner side at the bend exit.

When the Prandtl number increases, the thickness of the conduction sub-layer, the thermal equivalent of the viscous sub-layer, is reduced, making the coefficient of wall heat flux more sensitive to variations in near-wall turbulence and consequently its prediction more sensitive to this phenomenon. The latter is evident in the comparisons of Figure 8, that shows the measured and computed variation of the side-averaged Nusselt number for Pr=5.9. The under-prediction of the upstream levels suggests that the experimental entry conditions were not thermally fully developed. Within and downstream of the turn, in contrast to the comparisons at the lower Prandtl number, the zonal models, especially the EVM, return a reasonable variation, though in the middle of the turn the Nusselt number is over-predicted. The low-Re EVM models over-predict the Nusselt number at the middle of the turn and also show a severe dip at the bend exit, not present in the measurements. Both these predictive deficiencies are less severe in the basic low-Re DSM closures, with the prediction of the

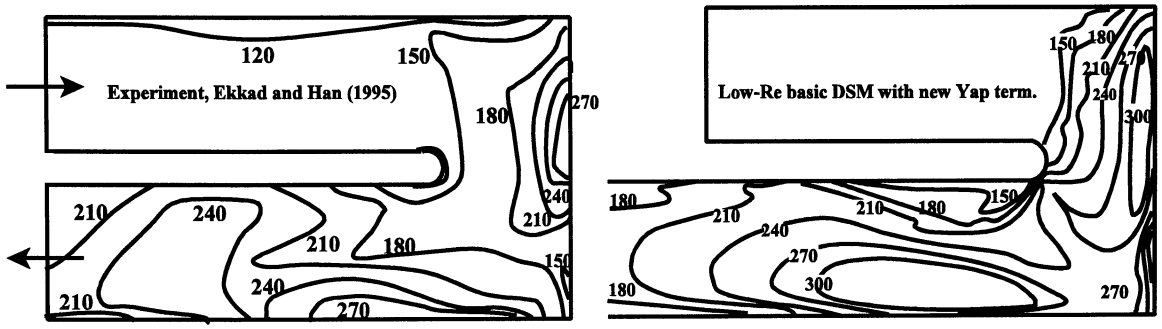

Figure 7. Comparisons of local Nusselt number along the flat wall. Re=60,000 and Pr-0.72.

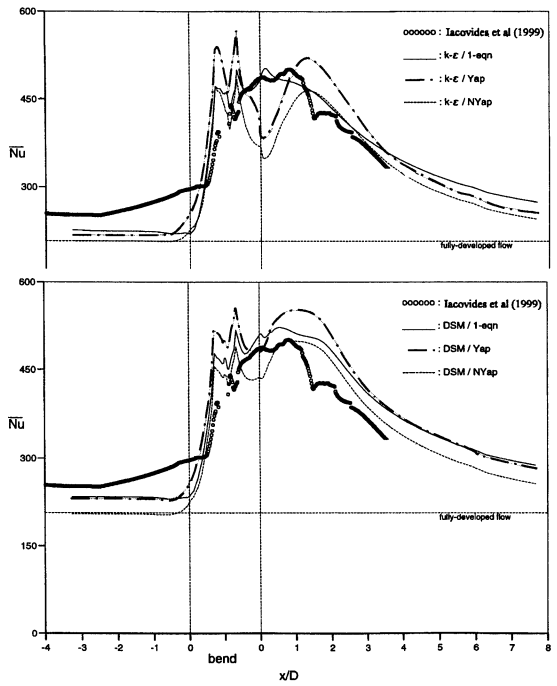

Figure 8. Comparisons of the axial variation of the side-averaged Nusselt number along the flat wall. Re=36,000 and Pr=5.9

DSM closure with the differential Yap term being notably closer to the measured distribution.

CONCLUDING REMARKS

The comparisons shows that all turbulence models return similar mean flow fields, suggesting that the mean flow development is mainly influenced by mean flow parameters, such as pressure gradients, rather than the turbulence field. The main flow features are reproduced, but the secondary motion in the second half of the turn is not well predicted, while the size of the exit separation bubble is under-predicted. Turbulence levels in the second half of the bend are under-predicted, but this must at least be partly caused by the flow instabilities and indeed the lack of flow symmetry within the bend, reported by the experimentalists. The predictions of Nusselt number are found to be sensitive to the modelling of both near-wall turbulence and turbulence anisotropy. Using the variation in side-averaged Nusselt number as a guide, for air (Pr=0.72), the low-Re models are superior to the zonal models, though the Craft realisable DSM model does not produce any additional improvements in comparison to the basic low-Re DSM. With water (Pr=5.9), the average Nu predictions of the zonal models, especially the EVM, move closer to the measurements, while among the low-Re models only the basic DSM model with the differential Yap term returns reliable predictions. It thus appears that only the low-Re basic DSM produces reliable Nusselt number predictions for the range of Prandtl numbers examined.

REFERENCES

Bo T, Iacovides H and Launder B E, 1995, "Convective discretization schemes for the turbulence transport equations in flow predictions through sharp U-bends", Int. J. Num. Meth. Ht & Fl Fl, **5**, pp. 33-48.

Choi Y-D, Iacovides H and Launder B E, 1989, "Numerical comp. of turb. flow in a square-sectioned 180-deg bend.", ASME J Fl Engrg, **111**, pp 59-68.

Craft, T. J, 1998, "Prediction of heat transfer in turbulent stagnation flow with a new second-moment closure", Proc. 2nd Int. Conf. On Turbulent Heat transfer, **2**, 4.25-4.25, Manchester, UK.

Ekkad S.V and Han J. C, 1995, "Local heat transfer distributions near a sharp 180° turn of a two-pass smooth square channel using a transient liquid crystal image technique", J. of Flow Visualization and Image Processing, **2**, pp. 285-297.

Iacovides H (1999). "The computation of turbulent flow through stationary and rotating U-bends of with rib-roughened surfaces. "Int. J. on Numerical Methods in Fluids, **29**,865-876.

Iacovides, H, Jackson, DC, Kelemenis G., Launder BE and Yuan Y-M, 1999, "Experiments on local heat transfer in a rotating square-ended U-bend", Int. J. of Heat and Fluid Flow, **20**, pp. 302-310.

Iacovides H, Launder BE and Li H-Y, 1996a, "Application of a Reflection-Free DSM to Turbulent Flow and Heat Transfer in a Square-Sectioned U-Bend.", Int. J. of Expt. Thermal and Fluid Science, **13**, 419-429, 1996.

Iacovides H, Launder B.E & Li H-Y, 1996b, "The computation of flow development through stationary and rotating U-ducts of strong curvature", Int. J. Heat and Fluid Flow, **17**, pp. 22-33.

Iacovides H and Raisee M, 1999, "Recent progress in the computational flow and heat transfer in internal cooling passages of turbine blades", Int. J. of Heat and Fluid Flow, **20**, pp. 320-328.

Metzger DE. and Sahm MK., 1986, "Heat transfer around sharp 180° turns in smooth rectangular channels", ASME J. Heat transfer, **108**, pp. 500-506.

Rigby D. L, Ameri A. A, 1996, "Internal passage heat transfer prediction using multi block grids and k-ω turbulence model", ASME Paper, 96-GT-188.

Wolfshtein M, 1969, "The velocity and temperature distribution in one-dimensional flow with turbulence augmentation and pressure gradient.", Int. J. Heat and Mass Transfer, **12,** 301.

Yap, C.R., 1987, "Turbulent heat and momentum transfer in recirculation and impinging flows", PhD Thesis, Mechanical Engineering Dept., UMIST.